

Article

Controlling Laser Irradiation with Tissue Temperature Feedback Enhances Photothermal Applications: Ex-Vivo Evaluation on Bovine Liver

Özgür Kaya ^{1,*} , İpek Düzgören ¹, İnci Çilesiz ²  and Murat Gülsoy ¹ ¹ Institute of Biomedical Engineering, Boğaziçi University, Kandilli Campus, Üsküdar, Istanbul 34684, Turkey² Biomedical Engineering, Istanbul Technical University, Ayazağa Campus, Maslak, Istanbul 34469, Turkey

* Correspondence: ozgur.kaya1@boun.edu.tr

Abstract: Achieving repeatable and successful results without causing excessive collateral damage is of paramount importance for photothermal laser applications. Predetermined laser parameters cannot ensure patient safety and treatment success due to variance between optical and thermal characteristics among subjects. Controlling laser irradiation with tissue temperature feedback is the current gold standard for various photothermal treatments (PTT) which are rate processes described by the Arrhenius temperature integral. This study establishes the validity of our low-cost design that makes tissue surface temperature control during photothermal laser applications more accessible in resource limited clinical environments. We demonstrated the practical performance and potential of our system with ex-vivo bovine liver irradiation using an ytterbium fiber laser ($\lambda = 1071$ nm) with two independent variables: laser power (3.4 W; 6.8 W; 10.2 W) and target surface temperature (55 °C, 65 °C and 75 °C). Our system efficiently maintained tissue surface temperatures at target values in all laser power groups. In contrast, fixed-dose application groups displayed a high final temperature range and variation in the control experiment. Temperature–time responses of samples varied significantly, in agreement with a wide range of optical and thermal coefficients. Long exposure duration groups (lower power, higher target temperature) displayed more radical differences suggesting a dominance of optical and thermal characteristics over the response. The low-cost surface-temperature-controlled medical laser system we have developed is capable of ensuring the success and reproducibility of PTT modalities and patient safety.

Keywords: temperature regulation; laser control; medical laser treatment; photothermal interactions



Citation: Kaya, Ö.; Düzgören, İ.; Çilesiz, İ.; Gülsoy, M. Controlling Laser Irradiation with Tissue Temperature Feedback Enhances Photothermal Applications: Ex-Vivo Evaluation on Bovine Liver. *Appl. Sci.* **2023**, *13*, 237. <https://doi.org/10.3390/app13010237>

Academic Editor: Hossam S. Abbas

Received: 30 November 2022

Revised: 19 December 2022

Accepted: 20 December 2022

Published: 24 December 2022



Copyright: © 2022 by the authors. Licensee MDPI, Basel, Switzerland. This article is an open access article distributed under the terms and conditions of the Creative Commons Attribution (CC BY) license (<https://creativecommons.org/licenses/by/4.0/>).

1. Introduction

Medical laser applications in the photothermal region rely heavily on heat generation to achieve desired thermo-physiological effects [1,2]. Achieved physiological effects are tissue temperature dependent. Tissue temperature, in turn, is a function of generated heat, optical, and thermal properties of the tissue including perfusion characteristics [3]. Depending on the medical procedure, it is necessary to ensure that some of these thermo-physiological effects are generated while preventing some others. Laser tissue welding (LTW) [4–8], ablation of soft tissues [9,10], photocoagulation and photothermal denaturation [11], angioplasty [12,13], treatment of granulation tissues [14], cartilage regeneration [15], and reshaping [16] are among possible medical photothermal laser treatments (PTT).

Thermo-physiological interactions occur within a narrow temperature range. Any deviation from this range may result in treatment failure or excessive thermal damage [6]. For instance, photothermal treatment of granulation tissue aims to trigger apoptosis by hyperthermia (45–50 °C) induced heat shock protein production without causing necrosis (>50 °C) [14]. Another example for a highly temperature sensitive application is LTW. Optimally, LTW requires temperatures between 65 °C and 70 °C (skin tissue) to ensure collagen denaturation (>63 °C for treatment success) [17]. Keeping the tissues at this

temperature range for a moderate duration of time (ranging from 0.06 s to minutes) also prevents excessive thermal damage (coagulative necrosis, heat fixation), which results in scarring and prolonged recovery time [18]. Currently, both treatment of granulation tissue and LTW are experimental procedures, not regularly used in clinical environment due to reproducibility and safety issues.

Thermal and optical characteristics of tissues vary among individuals and can change even within the same individual over time [3,19]. Dosimetry studies are widely used for determining laser parameters and exposure durations for PTT. While providing generally satisfactory laser parameters for treatments, dosimetry studies conducted in controlled environments of laboratories (using rather uniform research animals) do not ensure optimal results for all subjects. A predetermined dose may result in successful treatments in the majority of subjects, but may also lead to treatment failure and/or excessive thermal damage in some subjects. Therefore, conducting PTT with real-time tissue temperature feedback control is necessary.

A tissue temperature controlled medical laser system ensures treatment success and standardization, as well as patient safety. It also compensates for inexperienced operators increasing reproducibility of results for current PTT modalities used in the clinic. Consequently, a temperature controlled system may endorse the translation of experimental laser techniques (e.g., LTW, granulation tissue treatment, cartilage reshaping), which currently are limited to the controlled environment of the laboratory, into regular clinical practice. Such a system may also be used in the research of thermal characteristics of tissues and development of new laser treatment techniques. Additionally, it can be used for preventing undesirable temperature increase during photochemical procedures (e.g., photodynamic therapy and low-level laser therapy), which are non-thermal processes by nature [20,21].

Various research groups utilized different techniques to develop temperature measurement and control systems for medical laser applications [4–7,9,11,12,16,22–25]. These systems excel at different aspects of temperature control (e.g., fast response time, high accuracy, high spatial resolution) but mostly share a common drawback: the requirement of multiple and costly apparatus that are complicated to use in the clinical environment.

Our aim was to design a low-cost, compact and simple to use non-contact temperature controlled medical laser system that can be easily implemented in a resource limited (lacking expensive control systems and the highly skilled technical staff to operate these systems) clinical environment. We have developed this limited-resource-compatible system using a high SNR infrared thermocouple (IRT/c) sensor to measure the blackbody radiation emanating from the surface of the tissue [26]. The total cost of this system including the microcontroller board, optical opto-electronical, and -mechanical components and excluding the laser source and driver is ca. 300 USD (single unit retail prices).

Building on Kaya and Gülsoy (2016), this study evaluates the practical performance of our tissue-temperature-controlled laser system in comparison to a fixed-dose laser application using higher power densities on the bovine liver tissue to provide an example for photothermal liver tumor treatments.

2. Materials and Methods

Apart from being a good model for human liver applications, using bovine liver as tissue sample provided several other advantages. Bovine liver is easy to acquire and conforms with other soft tissues regarding water content. Furthermore, using *ex vivo* tissue samples acquired from a slaughterhouse on different days enabled us to match clinical conditions (widely varying optical and thermal characteristics among subjects) in contrast to the more uniform properties among laboratory animals. Near-IR, and specifically Nd:YAG ($\lambda = 1064$ nm) lasers, are commonly used for photothermal applications due to their ideally balanced tissue penetration and absorption characteristics [27,28]. For this purpose, we used a near-IR laser with a similar center wavelength ($\lambda = 1071$ nm).

2.1. Non-Contact Temperature Controlled Medical Laser System

The experimental setup is composed of a laser ($\lambda = 1071$ nm, Ytterbium Fiber Laser, YLM-20SC, IPG Photonics, Oxford, MA, USA), laser delivery optics designed for a converging beam with a Gaussian profile, providing a spot diameter of 3.5 mm ($1/e^2$) at the application distance (40 mm), and an IRt/c temperature measurement and laser control system as illustrated in Figure 1. We used a commercially available IRt/c sensor (MLX90614ESF-BCC, Melexis NV, Leper, Belgium) with a spectral bandwidth of 5.5–12 μm in our temperature measurement system; therefore, the system does not get affected by the laser irradiation. We also utilized a $1/2''$ Lens Tube and an AR coated (3–11 μm) ZnSe lens (ZnSe10, Crystran Ltd., Dorset, UK) to house the IRt/c sensor and to convert the diverging measurement cone of the sensor into a converging measurement cone. We calibrated our temperature measurement system using a NIST certified blackbody source (BB702, Omega Engineering, Norwalk, CT, USA). The IRt/c system takes average surface temperature measurements from a center weighted 3.6 mm diameter spot at 41 mm focal distance. It operates at 57 ms refresh time with 1 $^\circ\text{C}$ accuracy and 0.02 $^\circ\text{C}$ resolution. Our previous work contains details on characterization methods for determining system specifications [26]. We assumed that the emissivity of the tissue is equal to the emissivity of water ($\epsilon = 0.96$). The IRt/c sensor assembly is attached to the side of the laser delivery optics at an oblique angle to perfectly coincide laser application and temperature measurement spots without interfering with the laser beam as depicted in Figure 1. We have used an ON-OFF feedback control mechanism for ensuring fast response of the system. The laser exposure is modulated using a TTL signal generated by the TI MSP-EXP430F5529LP microcontroller board, which also reads out the IRt/c sensor via an I²C interface. This microcontroller feeds the real-time temperature data and the laser control signal to a computer via a Bluetooth connection for display and storage.

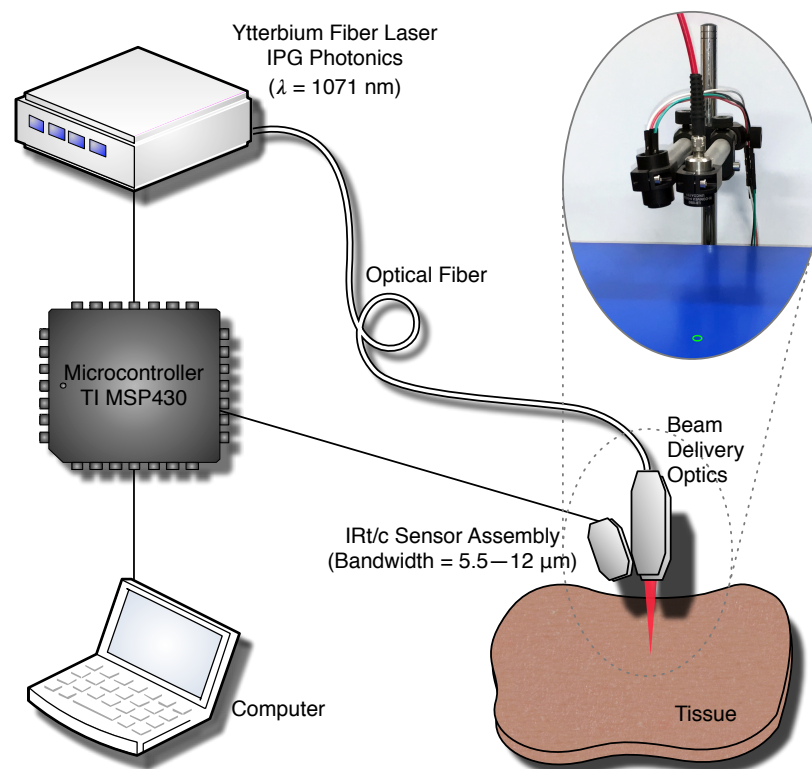


Figure 1. Schematic and photo of the experiment setup. The laser delivery optics (Gaussian profile, $\varnothing_{laser} = 3.5$ mm @ $d = 40$ mm) and the temperature measurement system ($\varnothing_{measurement} = 3.6$ mm @ $f = 41$ mm) are in an off-axis alignment configuration.

2.2. Photothermal Irradiation of Bovine Liver Tissue

2.2.1. Groups

We used 3 different laser powers and 3 different target temperatures (55 °C, 65 °C and 75 °C), corresponding to 9 experiment groups ($n = 16$), in surface temperature controlled mode. We also conducted a fixed-dose application as a control experiment which, additionally, enabled us to show the difference between tissue surface temperatures reached at the end of the exposure within the same group. We used the same 3 power levels in the fixed-dose application. The fixed-dose of each group ($n = 16$) in the control experiment was determined from the temperature controlled application data. We have computed the total exposure duration for each sample using the recorded laser control signal data and averaged this value within each application group to compute the fixed exposure duration, hence the fixed-dose (by multiplying the duration with the laser power) for each control group as provided in Table 1. The power levels 3.4 W, 6.8 W and 10.2 W correspond to average power densities of 35 W/cm², 71 W/cm², and 106 W/cm², respectively, for the Gaussian profile laser spot.

Table 1. Average dose delivered in the temperature controlled (experiment) groups and their equivalent exposure duration for the given power setting in fixed-dose (control) groups.

	55 °C	65 °C	75 °C
3.4 W	83.4 J (24.54 s)	142.5 J (41.91 s)	215.1 J (63.26 s)
6.8 W	53.5 J (7.87 s)	74.3 J (10.93 s)	104.0 J (15.29 s)
10.2 W	41.7 J (4.09 s)	64.5 J (6.32 s)	79.8 J (7.82 s)

2.2.2. Sample Preparation

Bovine livers were acquired from the slaughterhouse and stored at 4 °C until the procedure. On the experiment day, the liver of each animal was dissected to end up with 9 or 18 samples (corresponding to 1 or 2 samples from the same animal for each experiment group) of ca. 3 cm × 3 cm × 1.5 cm. This size was sufficient for providing a smooth and even surface for the target area, away from fascia and veins. The samples were packaged in aluminum foil for preventing desiccation and assigned randomly to groups. After reaching room temperature (ca. 23 °C), they were placed on a lab jack for irradiation.

2.2.3. Irradiation Procedure

The lab jack height was adjusted for aligning the top surface of the tissue sample with the laser spot and temperature measurement spot in order to ensure perfect overlapping of irradiation spot center with the temperature measurement spot center. The sample was positioned with the help of a visible guide beam to target a locus away from veins and fascia. Laser irradiation procedure was initiated from the computer by first starting the temperature data recording and then turning CW laser exposure on. In the temperature-controlled applications, once the tissue surface temperature reached the target value, the microcontroller modulated the laser exposure to maintain the target temperature for 5 s and then ceased the irradiation. The 5 s duration was chosen because it provides sufficient time at the target temperature for thermal effects to be manifested without causing significant desiccation. In the fixed-dose applications (control experiment), the CW laser irradiation was maintained until the end of the predetermined duration for each fixed-dose group.

3. Results

Figures 2 and 3 reveal the raw (unfiltered) and superimposed temperature measurement data of all samples within each application group in temperature-controlled and fixed-dose applications, respectively. Further descriptive quantitative data are provided in Table 2 for the temperature-controlled application and in Table 3 and Figure 4 for the fixed-dose application.

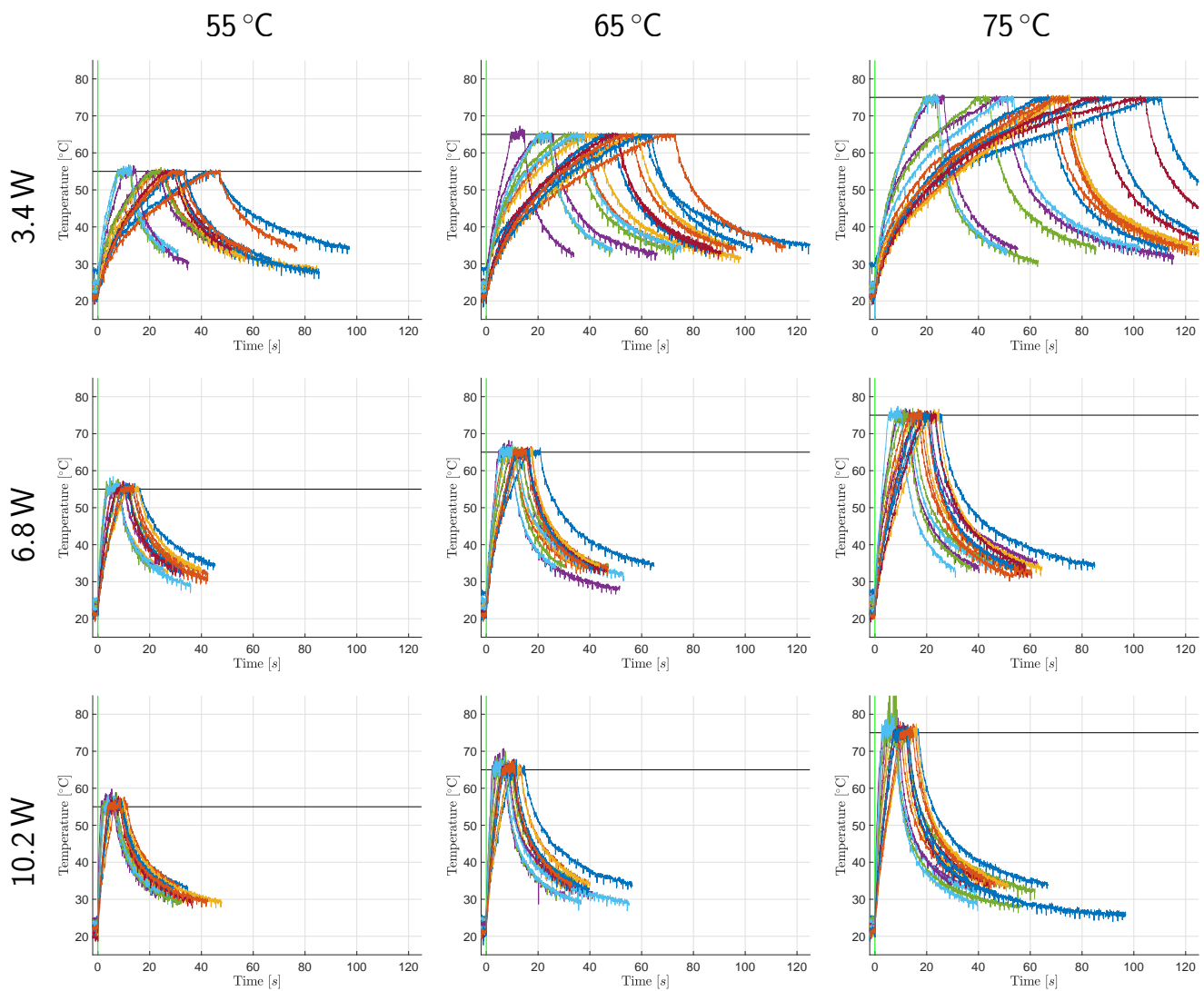


Figure 2. Temperature monitoring data of surface temperature controlled laser irradiation. The temperature–time response graphs (each individual sample represented with a different curve color) within each group are superimposed. The horizontal black lines and the vertical green lines represent the target temperature values and the laser emission commencement marks, respectively.

Table 2. Descriptive temperature values for the surface temperature controlled application: The mean (μ) and standard deviation (σ) values of maximum (T_{max}), minimum (T_{min}), mean (μ_T) and standard deviation (σ_T) values of the tissue surface temperature during the 5 s-period at the target value.

P_{laser}	T_{target}	$\mu_{T_{5s}}(\mu \pm \sigma)$ [°C]	$\sigma_{T_{5s}}(\mu \pm \sigma)$ [°C]	$T_{min}(\mu \pm \sigma)$ [°C]	$T_{max}(\mu \pm \sigma)$ [°C]
3.4 W	55 °C	54.6 ± 0.1	0.6 ± 0.1	52.8 ± 0.4	55.8 ± 0.5
	65 °C	64.5 ± 0.1	0.5 ± 0.1	62.8 ± 0.4	65.6 ± 0.5
	75 °C	74.4 ± 0.1	0.6 ± 0.1	72.6 ± 0.7	75.5 ± 0.2
6.8 W	55 °C	55.0 ± 0.2	0.7 ± 0.1	52.9 ± 0.5	57.0 ± 0.6
	65 °C	64.8 ± 0.2	0.8 ± 0.2	62.6 ± 0.6	66.6 ± 0.6
	75 °C	74.6 ± 0.1	0.8 ± 0.1	72.4 ± 0.5	76.4 ± 0.5
10.2 W	55 °C	55.3 ± 0.2	1.0 ± 0.2	52.8 ± 0.5	57.8 ± 0.9
	65 °C	65.1 ± 0.3	1.1 ± 0.3	62.3 ± 0.7	67.8 ± 1.2
	75 °C	74.9 ± 0.8	1.3 ± 0.8	71.8 ± 1.3	77.5 ± 1.1

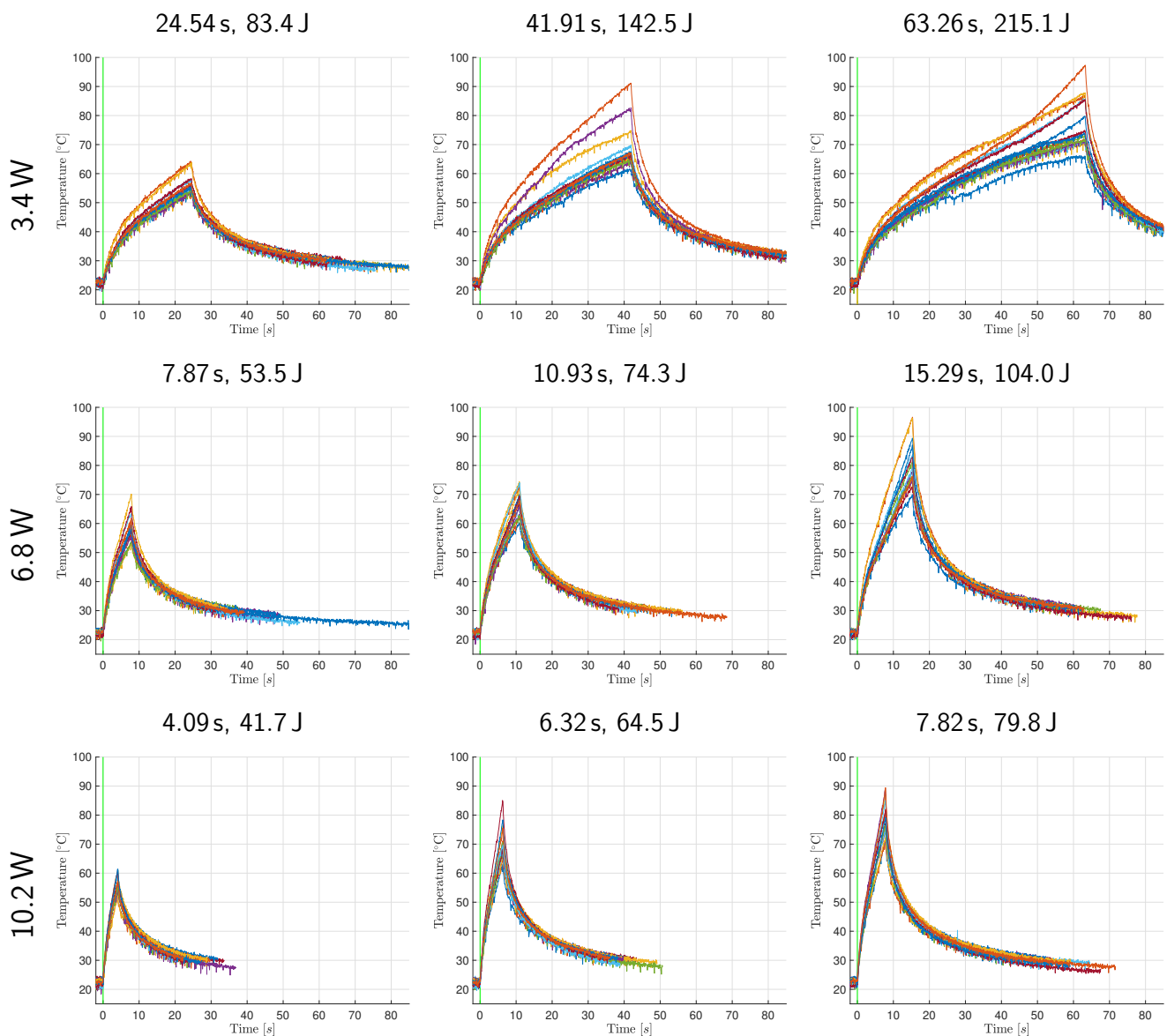


Figure 3. Temperature monitoring data of the fixed-dose application. The temperature–time response graphs (each individual sample represented with a different curve color) within each group are superimposed. The vertical green lines represent the laser emission commencement marks.

Table 3. Descriptive temperature values for the fixed-dose application: The mean (μ), standard deviation (σ), range ($max - min$), maximum (max) and minimum (min) values of the achieved tissue surface temperature at the end of laser exposure (T_{final}).

P_{laser}	$t_{exposure}$	E	$T_{final}(\mu \pm \sigma)$ [°C]	$T_{final}(max)$ [°C]	$T_{final}(min)$ [°C]
3.4 W	24.54 s	83.4 J	56.5 ± 3.2	64.3	53.8
	41.91 s	142.5 J	69.5 ± 7.5	91.2	61.6
	63.26 s	215.1 J	77.5 ± 8.7	97.4	66.2
6.8 W	7.87 s	53.5 J	59.0 ± 4.6	70.1	53.1
	10.93 s	74.3 J	67.8 ± 4.3	74.5	60.2
	15.29 s	104.0 J	81.0 ± 7.9	96.6	70.0
10.2 W	4.09 s	41.7 J	57.5 ± 2.9	61.4	52.2
	6.32 s	64.5 J	70.9 ± 5.5	85.1	63.0
	7.82 s	79.8 J	79.3 ± 6.1	89.4	71.0

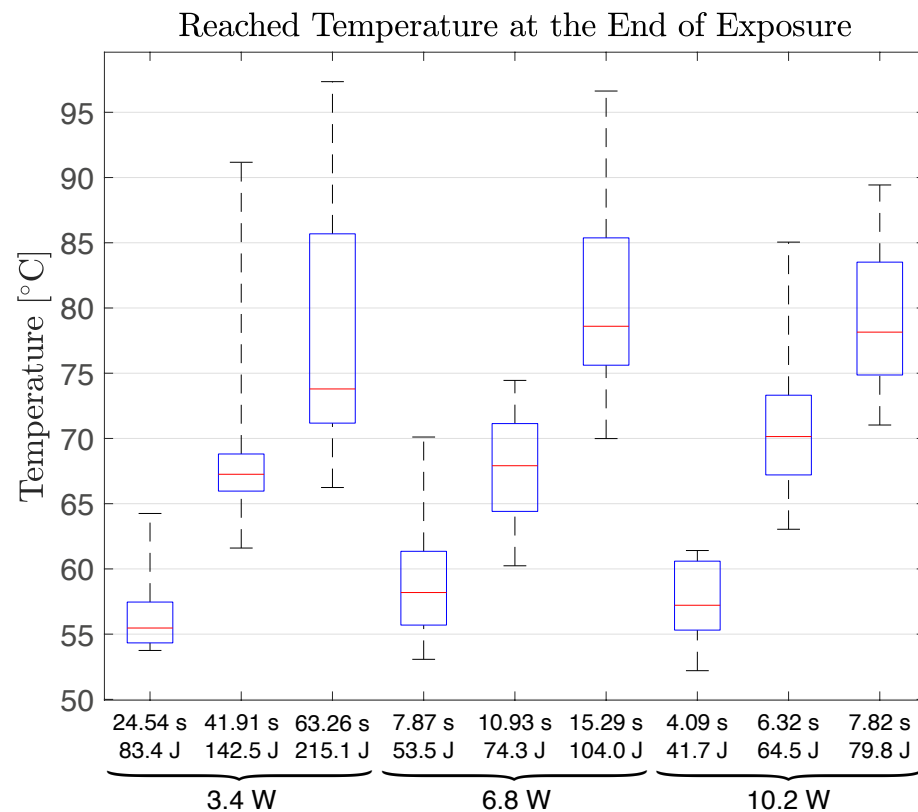


Figure 4. Box and whiskers plot of the tissue surface temperature reached at the end of exposure in the fixed-dose application. The red horizontal lines are the group medians. The blue boxes mark the interquartile ranges. The whiskers indicate the whole data range.

4. Discussion

Temperature–time responses of samples vary significantly within the same application group as depicted in Figures 2 and 3. These results confirm our initial assumptions regarding the non-uniformity of optical and thermal characteristics among subjects and show that temperature control is necessary for photothermal medical laser applications. As illustrated in Figure 2, our system can successfully control the tissue surface temperature during laser exposure. Mean tissue surface temperatures during the 5 s temperature controlled period do not deviate from the target value more than 0.6 °C on average. The maximum and minimum temperatures observed during this period also remain within a narrow range (4.1 °C on average) demonstrating the temperature stability our system can provide. This finding is also supported by the small magnitudes of the standard deviation values in Table 2.

Among a total of 144 samples in the temperature-controlled applications, only two samples of $P_{\text{laser}} = 10.2 \text{ W}$ & $T_{\text{target}} = 75 \text{ °C}$ group displayed anomalies. One sample contained fascia tissue underneath the target area, and the temperature increase caused it to contract, moving the laser irradiated surface in and out of the measurement spot. The fact that our system is a confocal *but* not a coaxial optical setup caused measurement errors due to the alteration of the target surface distance to the probe. Off-axis alignment requires a precise and constant application distance. Use of a mechanical spacer or another technology (e.g., a distance sensor) to ensure the required target to probe distance is necessary for handheld operation. The other sample experienced a high rate of temperature change ($>20 \text{ °C/s}$) and has undergone partial carbonization at the center of the laser spot, even though the highest measured temperature was below 90 °C. Considering the Gaussian laser beam generates higher temperatures at the center of the spot, partial carbonization at that location is natural.

On the other hand, fixed-dose application results display increasing tissue surface temperatures until the end of the procedure (cessation of irradiation), as shown in Figure 3, resulting in a wide range of final temperatures within each group, as presented in Figure 4. These results prove that a fixed-dose cannot be relied upon to ensure treatment success (reaching desired temperature) while preventing excessive thermal damage in the clinical conditions due to the high temperature sensitivity of physiological effects generated in PTT.

Arrhenius temperature integral suggests that the progression of thermal damage is linear for constant tissue temperatures and exponential for linearly increasing tissue temperatures [6]. As a consequence, swiftly reaching a target value (depending on the desired physiological effect) and maintaining the tissue temperature at that value renders the progression of thermal damage a linear function of time. Our system can be used to constrain tissue surface temperature during laser exposure to control progression of thermal damage while guaranteeing the induction of desired physiological effects and preventing undesirable outcomes (e.g., carbonization, heat fixation, coagulative necrosis).

As the tissue is exposed to laser light, its temperature increases and a multitude of phenomena occur simultaneously [29]. Coagulation and denaturation of proteins change the optical properties of the tissue [6,19,30]. Moreover, the absorption coefficient of water at the ytterbium fiber laser wavelength ($\lambda_{center} \approx 1070$ nm) decreases with increasing temperature [31]. The water content of the tissue may change due to evaporation induced dehydration (in conditions with very high temperatures or extended exposure durations). As water content decreases, thermal conductivity of tissue reduces [32]. Optical and thermal properties of the tissue dynamically change with its temperature and hydration level during laser irradiation [3,6,19].

In Figure 2, the lower laser power groups display a higher variation in their temperature increase curves. It seems that optical and thermal differences of samples dominate the temperature–time response of tissue when laser power is low. In addition, low power groups require longer to reach the target temperature. Thus, the tissue has more time to undergo the optical and thermal property changes elaborated above. The same observation and deduction are also valid, albeit to a lesser extent, for higher target temperature groups corresponding to longer exposure durations. Low power and longer duration groups in the fixed-dose application also display a higher variation in their temperature–time response curves. This resulted in higher final temperature ranges as presented in Table 3.

It is important to note that the emissivity, ϵ , can be a source of error in infrared temperature measurements. The accuracy and thus the performance of this system rely on the assumption of constant tissue emissivity that is equal to the emissivity of water. However, there is a linear relationship between the measured temperature and the fourth root of $1/\epsilon$ (inverse of emissivity), which corresponds to negligible measurement errors unless the change in emissivity is dramatic.

Another important point is that the infrared temperature measurement systems collect blackbody radiation only from the top 25–30 μm and the laser wavelength we have used ($\lambda = 1071$ nm) has a penetration depth of ca. 2–6 mm similar to Nd:YAG. This phenomenon may reduce the effectiveness of IR thermometrical laser control systems like ours and should be taken into consideration when using different irradiation wavelengths (This IR temperature measurement system should not be used with irradiation wavelengths close to or within the measurement bandwidth of 5.5–12 μm to avoid significant measurement errors). However, in the clinical setting, the perfusion of the tissue should have a cooling effect mainly below the tissue surface and we expect that the deeper tissue temperature would be lower than the surface temperature, practically eliminating the technical limitation of our system especially for laser wavelengths with less tissue penetration (until the 25 μm limit).

We have even conducted a thermal denaturation area study (available in the supplementary material) which supports our findings reported here.

Study Limitations

Even though our IRt/c system is calibrated, one limitation of this study is the lack of a secondary temperature measurement system for confirming our results. We abstained from using a contact requiring temperature measurement method to avoid changing the thermal dissipation characteristics of the tissue and interfering with the laser exposure. Unfortunately, a high resolution thermal camera with a fast temperature response was not available at hand.

5. Conclusions

The surface-temperature-controlled medical laser system developed in our laboratory is capable of ensuring the success and reproducibility of PTT modalities and patient safety even when using a sample population representative of wide optical and thermal property ranges encountered in clinical conditions. Our system successfully maintains tissue surface temperatures at required target values to induce desired thermo-physiological effects and prevents excessive thermal damage even when using different laser powers. It comprises relatively inexpensive components that perform efficiently even when using the simplest control method. It has an easy to operate, simple design that can be set up and used in the clinical environment in an appropriate enclosure without requiring complicated training. Thus, it may accelerate and enable the translation of novel photothermal laser applications currently confined to the controlled and uniform conditions of the laboratory (e.g., laser-tissue welding, PTT of granulation tissue, cartilage reshaping) into the clinic by rendering them more successful, reproducible, and safe even for a wide range of subjects which cannot be provided by manual dosimetry (surgeon's decision) or fixed-dosimetry. Additionally, researchers may use our system for investigating and developing new, and improving pre-existing, photothermal laser applications on various biological tissues by monitoring tissue surface temperature, controlling laser exposure, and facilitating gathering of information of related parameters (i.e., thermal characterization of tissues).

Using the temperature monitorization capability of our system, we noticed that low laser power values accentuate the effect idiosyncratic differences of optical and thermal properties of tissues have on their temperature–time responses. This interaction between low laser power and idiosyncratic properties of tissues led to a wider range of exposure durations (required to reach target temperatures) in temperature-controlled laser irradiation.

Regulating photothermal medical laser applications by tissue temperature feedback is currently the gold standard of the trade. Our future work will focus on implementing laser power modulation and improving the control algorithm to monitor and manipulate the rate of tissue surface temperature increase. We will also conduct experiments to demonstrate the *in vivo* effectiveness of our system. Investigation of methods for determining tissue emissivity to ensure measurement accuracy and reliability is another course of further research.

Supplementary Materials: The following supporting information can be downloaded at: <https://www.mdpi.com/article/10.3390/app13010237/s1>, Figure S1: Box and whiskers plot of thermal denaturation diameters and depths; Figure S2: Exemplary bovine liver photothermal denaturation photographs; Table S1: Results of post hoc tests using Scheffe's procedure after one-way ANOVA of thermal denaturation diameter and depth values. References [33–36] are cited in the supplementary materials.

Author Contributions: Conceptualization, Ö.K. and M.G.; methodology, Ö.K. and M.G.; software, Ö.K.; formal analysis, Ö.K. and İ.D.; investigation, Ö.K. and İ.D.; resources, Ö.K. and M.G.; data curation, Ö.K.; writing—original draft preparation, Ö.K.; writing—review and editing, İ.Ç. and M.G.; visualization, Ö.K.; supervision, İ.Ç. and M.G.; project administration, Ö.K. and M.G.; funding acquisition, Ö.K. and M.G. All authors have read and agreed to the published version of the manuscript.

Funding: This research was funded internally by the Boğaziçi University Research Fund Grant No. BAP-8500 14XM2.

Institutional Review Board Statement: Ethical review and approval were waived for this study because ex vivo tissues were acquired from an abattoir.

Informed Consent Statement: Not applicable.

Data Availability Statement: The data presented in this study are available on request from the corresponding author.

Acknowledgments: The authors would like to thank Esin Öztürk Işık for guidance on statistical analysis in the study and Mehmet Emre Hatipoğlu for constructive criticism of the manuscript.

Conflicts of Interest: The authors declare no conflict of interest.

Abbreviations

The following abbreviations are used in this manuscript:

PTT	Photothermal therapy
LTW	Laser tissue welding
IRt/c	Infrared thermocouple
SNR	Signal to noise ratio
USD	United States Dollar
Near-IR	Near infrared
Nd:YAG	Neodymium-doped yttrium aluminum garnet
ZnSe	Zinc selenide
NIST	National Institute of Standards and Technology
TTL	Transistor–transistor logic
I ² C	Inter-Integrated circuit
CW	Continuous wave

References

- Niemz, M.H. Laser-Tissue Interactions: Fundamentals and Applications. In *Laser-Tissue Interactions: Fundamentals and Applications*, 3rd ed.; Springer Science & Business Media: Berlin/Heidelberg, Germany, 2007; pp. 58–80. [\[CrossRef\]](#)
- Thomsen, S.; Pearce, J.A. Thermal Damage and Rate Processes in Biologic Tissues. In *Optical-Thermal Response of Laser-Irradiated Tissue*, 2nd ed.; Welch, A.J., Van Gemert, M.J., Eds.; Springer: Dordrecht, The Netherlands, 2011; pp. 487–549. [\[CrossRef\]](#)
- Valvano, J.W. Tissue thermal properties and perfusion. In *Optical-Thermal Response of Laser-Irradiated Tissue*, 2nd ed.; Welch, A.J., Van Gemert, M.J., Eds.; Springer: Dordrecht, The Netherlands, 2011; pp. 455–485. [\[CrossRef\]](#)
- Poppas, D.P.; Stewart, R.B.; Massicotte, J.M.; Wolga, A.E.; Kung, R.T.; Retik, A.B.; Freeman, M.R. Temperature-controlled laser photocoagulation of soft tissue: In Vivo evaluation using a tissue welding model. *Lasers Surg. Med.* **1996**, *18*, 335–344. [\[CrossRef\]](#)
- Stewart, R.B.; Benbrahim, A.; LaMuraglia, G.M.; Rosenberg, M.; L'Italien, G.J.; Abbott, W.M.; Kung, R.T. Laser assisted vascular welding with real time temperature control. *Lasers Surg. Med.* **1996**, *19*, 9–16. [\[CrossRef\]](#)
- Çilesiz, İ. Controlled Temperature Photothermal Tissue Welding. *J. Biomed. Opt.* **1999**, *4*, 327–336. [\[CrossRef\]](#)
- Spector, D.; Rabi, Y.; Vasserman, I.; Hardy, A.; Klausner, J.; Rabau, M.; Katzir, A. In Vitro large diameter bowel anastomosis using a temperature controlled laser tissue soldering system and albumin stent. *Lasers Surg. Med.* **2009**, *41*, 504–508. [\[CrossRef\]](#)
- Tabakoğlu, H.Ö.; Gülsoy, M. In Vivo comparison of near infrared lasers for skin welding. *Lasers Med. Sci.* **2010**, *25*, 411–421. [\[CrossRef\]](#) [\[PubMed\]](#)
- Ishihara, M.; Arai, T.; Sato, S.; Morimoto, Y.; Obara, M.; Kikuchi, M. Measurement of the Surface Temperature of the Cornea During ArF Excimer Laser Ablation by Thermal Radiometry With a 15-Nanosecond Time Response. *Lasers Surg. Med.* **2002**, *30*, 54–59. [\[CrossRef\]](#)
- Kopchok, G.E.; White, R.A.; Tabbara, M.; Saadatmanesh, V.; Peng, S.K. Holmium: YAG laser ablation of vascular tissue. *Lasers Surg. Med.* **1990**, *10*, 405–413. [\[CrossRef\]](#) [\[PubMed\]](#)
- Schlott, K.; Koinzer, S.; Ptaszynski, L.; Bever, M.; Baade, A.; Roeder, J.; Birngruber, R.; Brinkmann, R. Automatic temperature controlled retinal photocoagulation. *J. Biomed. Opt.* **2012**, *17*, 061223. [\[CrossRef\]](#)
- Small IV, W.; Celliers, P.; Kopchok, G.; Reiser, K.; Heredia, N.; Maitland, D.; Eder, D.; London, R.; Heilbron, M.; Hussain, F.; et al. Temperature Feedback and Collagen Cross-Linking in Argon Laser Vascular Welding. *Lasers Surg. Med.* **1998**, *13*, 98–105. [\[CrossRef\]](#)
- Singleton, D.; Paraskevopoulos, G.; Taylor, R.; Higginson, L. Excimer laser angioplasty: Tissue ablation, arterial response, and fiber optic delivery. *IEEE J. Quantum Electron.* **1987**, *23*, 1772–1782. [\[CrossRef\]](#)
- Landsberg, R.; DeRowe, A.; Katzir, A.; Shtabsky, A.; Fliss, D.M.; Gil, Z. Laser-induced hyperthermia for treatment of granulation tissue growth in rats. *Otolaryngol.—Head Neck Surg.* **2009**, *140*, 480–486. [\[CrossRef\]](#) [\[PubMed\]](#)

15. Sobol, E.; Shekhter, A.; Guller, A.; Baum, O.; Baskov, A. Laser-induced regeneration of cartilage. *J. Biomed. Opt.* **2011**, *16*, 080902. [[CrossRef](#)] [[PubMed](#)]
16. Wong, B.J.F.; Milner, T.E.; Anvari, B.; Sviridov, A.; Omel'chenko, A.; Bagratashvili, V.V.; Sobol, E.; Nelson, J.S. Measurement of radiometric surface temperature and integrated backscattered light intensity during feedback-controlled laser-assisted cartilage reshaping. *Lasers Med. Sci.* **1998**, *13*, 66–72. [[CrossRef](#)]
17. Simhon, D.; Halpern, M.; Brosh, T.; Vasilyev, T.; Ravid, A.; Tennenbaum, T.; Nevo, Z.; Katzir, A. Immediate tight sealing of skin incisions using an innovative temperature-controlled laser soldering device: In Vivo study in porcine skin. *Ann. Surg.* **2007**, *245*, 206–213. [[CrossRef](#)]
18. Coad, J.E. Thermal fixation: A central outcome of hyperthermic therapies (Invited Paper). In *Proceedings of the Thermal Treatment of Tissue: Energy Delivery and Assessment III*; Ryan, T.P., Ed.; SPIE: Bellingham, WA, USA, 2005. [[CrossRef](#)]
19. Barton, J.K. Dynamic changes in optical properties. In *Optical-Thermal Response of Laser-Irradiated Tissue*, 2nd ed.; Welch, A.J., Van Gemert, M.J., Eds.; Springer: Dordrecht, The Netherlands, 2011; pp. 321–349. [[CrossRef](#)]
20. Lim, H.S. Reduction of thermal damage in photodynamic therapy by laser irradiation techniques. *J. Biomed. Opt.* **2012**, *17*, 128001. [[CrossRef](#)]
21. Grandinetti, V.d.S.; Miranda, E.F.; Johnson, D.S.; de Paiva, P.R.V.; Tomazoni, S.S.; Vanin, A.A.; Albuquerque-Pontes, G.M.; Frigo, L.; Marcos, R.L.; de Carvalho, P.d.T.C.; et al. The thermal impact of phototherapy with concurrent super-pulsed lasers and red and infrared LEDs on human skin. *Lasers Med. Sci.* **2015**, *30*, 1575–1581. [[CrossRef](#)]
22. Çilesiz, İ.; Thomsen, S.; Welch, A.J. Controlled temperature tissue fusion: Argon laser welding of rat intestine in vivo, Part One. *Lasers Surg. Med.* **1997**, *21*, 269–277. [[CrossRef](#)]
23. Çilesiz, İ.; Thomsen, S.; Welch, A.J.; Chan, E.K. Controlled temperature tissue fusion: Ho:YAG laser welding of rat intestine in vivo, Part Two. *Lasers Surg. Med.* **1997**, *21*, 278–286. [[CrossRef](#)]
24. Tunç, B.; Gülsoy, M. Tm: Fiber laser ablation with real-time temperature monitoring for minimizing collateral thermal damage: Ex Vivo dosimetry for ovine brain. *Lasers Surg. Med.* **2013**, *45*, 48–56. [[CrossRef](#)]
25. Simhon, D.; Gabay, I.; Shpolyansky, G.; Vasilyev, T.; Nur, I.; Meidler, R.; Hatoum, O.A.; Katzir, A.; Hasmonai, M.; Kopelman, D. Temperature-controlled laser-soldering system and its clinical application for bonding skin incisions. *J. Biomed. Opt.* **2015**, *20*, 128002. [[CrossRef](#)]
26. Kaya, Ö.; Gülsoy, M. A non-contact temperature measurement system for controlling photothermal medical laser treatments. *Proc. SPIE* **2016**, *9706*, 97060K. [[CrossRef](#)]
27. Whelan, W.M.; Wyman, D.R. Dynamic modeling of interstitial laser photocoagulation: Implications for lesion formation in liver in vivo. *Lasers Surg. Med.* **1999**, *24*, 202–208. [[CrossRef](#)]
28. Jacques, S.L.; Rastegar, S.; Motamedi, M.; Thomsen, S.L.; Schwartz, J.A.; Torres, J.H.; Mannonen, I. Liver photocoagulation with diode laser (805 nm) versus Nd:YAG (1064 nm). *Proc. SPIE* **1992**, *1646*, 107–117. [[CrossRef](#)]
29. Diller, K.R. Laser generated heat transfer. In *Optical-Thermal Response of Laser-Irradiated Tissue*, 2nd ed.; Welch, A.J., Van Gemert, M.J., Eds.; Springer: Dordrecht, The Netherlands, 2011; pp. 353–397. [[CrossRef](#)]
30. Jaywant, S.M.; Wilson, B.C.; Patterson, M.S.; Lilge, L.D.; Flotte, T.J.; Woolsey, J.; McCulloch, C. Temperature-dependent changes in the optical absorption and scattering spectra of tissues: Correlation with ultrastructure. *Proc. SPIE* **1993**, *1882*, 218–229. [[CrossRef](#)]
31. Mullick, S.; Madhukar, Y.K.; Kumar, S.; Shukla, D.K.; Nath, A.K. Temperature and intensity dependence of Yb-fiber laser light absorption in water. *Appl. Opt.* **2011**, *50*, 6319–6326. [[CrossRef](#)] [[PubMed](#)]
32. Spells, K.E. The Thermal Conductivities of some Biological Fluids. *Phys. Med. Biol.* **1960**, *5*, 139. [[CrossRef](#)]
33. Anderson, R.R. Polarized light examination and photography of the skin. *Arch. Dermatol.* **1991**, *127*, 1000–1005. [[CrossRef](#)]
34. Beatty, C.J.; Thomsen, S.L.; Vos, J.A.; Coad, J. Practical pathology for thermal tissue applications. *Proc. SPIE* **2015**, *9326*, 932602. [[CrossRef](#)]
35. Thomsen, S.; Pearce, J.; Cheong, W.F. Changes in birefringence as markers of thermal damage in tissues. *IEEE Trans. Biomed. Eng.* **1989**, *36*, 1174–1179. [[CrossRef](#)]
36. Sherwood, M.E.; Flotte, T.J. Improved staining method for determining the extent of thermal damage to cells. *Lasers Surg. Med.* **2007**, *39*, 128–131. [[CrossRef](#)]

Disclaimer/Publisher's Note: The statements, opinions and data contained in all publications are solely those of the individual author(s) and contributor(s) and not of MDPI and/or the editor(s). MDPI and/or the editor(s) disclaim responsibility for any injury to people or property resulting from any ideas, methods, instructions or products referred to in the content.